THE JOURNAL OF BIOLOGICAL CHEMISTRY VOL. 283, NO. 1, pp. 416–426, January 4, 2008

TRPC4 in Rat Dorsal Root Ganglion Neurons Is Increased after Nerve Injury and Is Necessary for Neurite Outgrowth*

Received for publication, April 16, 2007, and in revised form, September 4, 2007 Published, JBC Papers in Press, October 10, 2007, DOI 10.1074/jbc.M703177200

Dongsheng Wu, Wenlong Huang, Peter M. Richardson, John V. Priestley, and Min Liu[1]

From the Neuroscience Centre, Institute of Cell and Molecular Sciences, Queen Mary University of London, London E1 2AT, United Kingdom

Canonical transient receptor potential (TRPC) receptors are Ca^{2+}-permeable cation channels that have a variety of physiological functions and may be involved in neuronal development and plasticity. We investigated the expression profile of TRPC channels in adult rat dorsal root ganglia (DRG) after nerve injury and examined the role of TRPC4 in neurite outgrowth in cultured DRG neurons. Sciatic nerve transection and microinjection of dibutyryl cAMP were employed to induce axonal regeneration *in vivo*. TRPC4 mRNA was significantly increased whereas TRPC1, TRPC3, TRPC6, and TRPC7 remained unaltered after nerve injury or dibutyryl-cAMP microinjection. The increases in TRPC4 transcript and protein were transient with maximal levels reached at 2 or 7 days, respectively. In addition, TRPC4 transcript in ND7/23 and NDC cells, hybrid cell lines derived from neonatal DRG and neuroblastoma, was substantially increased on differentiation, characterized by neurite outgrowth. In adult DRG, TRPC4 immunoreactivity was found in small and large neurons, and nerve injury increased the number of TRPC4-immunoreactive cells, particularly in large neurons. TRPC4 immunoreactivity was present in growth cones at various stages of DRG neurite outgrowth *in vitro*. Suppression of TRPC4 by a specific small interfering RNA or antisense significantly reduced the length of neurites in cultured DRG neurons. Expression of short hairpin RNA significantly down-regulated TRPC4 protein level and shortened neurite lengths in differentiated ND7/23 cells. The reduction in neurite lengths in ND7/23 cells was rescued by overexpression of human TRPC4. Our results suggest that TRPC4 contributes to axonal regeneration after nerve injury.

It has been recognized for years that Ca^{2+} is a critical mediator of the path finding and elongation of growing axons through its regulation of cytoskeletal molecules and membrane dynamics (1, 2). Several Ca^{2+}-permeable ion channels, including voltage-operated calcium channels, ligand-gated channels, and store-operated channels, contribute to Ca^{2+} transients in growing axons. Recently, members of the transient receptor potential (TRP)[2] family have been identified as new Ca^{2+} influx pathways. For example, TRPC1 homologue mediates Ca^{2+} increase and thus growth cone turning induced by the guidance cue of BDNF (brain-derived neurotrophic factor) and by the repellent factor of myelin-associated glycoprotein in *Xenopus* spinal neurons (3, 4). Thus, we asked whether TRPC channels might play a role in mammalian nerve regeneration after injury.

TRP receptors can be classified into seven subfamilies, TRPC, TRPV, TRPM, TRPN, TRPA, TRPP, and TRPML (5, 6). The mammalian TRPC (canonical) subfamily consists of seven members (TRPC1-TRPC7) that bear structural similarity to *Drosophila* TRP photoreceptors. TRPC channels serve a wide range of physiological functions ranging from proliferation of vascular smooth muscle (7) to mechanical sensory transduction (8). Although it remains controversial whether TRPC receptors function as store-operated Ca^{2+} channels, it is generally accepted that they are activated by $G\alpha_q$-coupled receptors and tyrosine kinase-linked receptors through phospholipase C activation or diacylglycerol production (6). For example, TRPC3 is activated in a phospholipase C-dependent manner following the activation of TrkB by BDNF in central nervous system neurons (9, 10).

Injury to the peripheral axons of primary sensory neurons induces changes in the cell bodies that support axonal regeneration. For example, the regrowth of injured axons in dorsal spinal roots or from dorsal columns of the spinal cord is enhanced strongly by a concomitant peripheral nerve injury (11, 12). Application of exogenous cAMP to DRG effectively mimics this conditioning effect both in *vitro* and in *vivo* (13–15). However, the molecular changes within injured neurons that mediate this growth potential are only partially understood. In the present study, we have investigated possible changes in the expression of TRPC genes after sciatic nerve transection and intra-ganglionic microinjection of db-cAMP. We have found a marked transient increase in TRPC4 transcript and protein in DRG cells following either treatment. The elongation of neurites in DRG neurons was significantly impaired when TRPC4 expression was suppressed by siRNA (small interfering RNA) or antisense. Thus, our data have revealed a close relationship between TRPC4 expression and axonal regeneration in adult DRG neurons.

EXPERIMENTAL PROCEDURES

Conditioning Nerve Lesion and Intra-ganglionic Injection—All experimental protocols were approved by the local animal

* This work was supported by grants from St. Bartholomew's and the Royal London Charitable Foundation. The costs of publication of this article were defrayed in part by the payment of page charges. This article must therefore be hereby marked "*advertisement*" in accordance with 18 U.S.C. Section 1734 solely to indicate this fact.

[1] To whom correspondence should be addressed: 4 Newark St., London E1 2AT, UK. Fax: 44-207-882-2180; E-mail: m.liu@qmul.ac.uk.

[2] The abbreviations used are: TRP, transient receptor potential; TRPC, canonical TRP receptor; hTRPC4, human TRPC4; db-cAMP, dibutyryl cAMP; DRG, dorsal root ganglion; siRNA, small interfering RNA; shRNA, short hairpin RNA; NGF, nerve growth factor; RT-PCR, reverse transcriptase PCR; PBS, phosphate-buffered saline; BDNF, brain-derived neurotrophic factor.

care committee in accordance with UK Home Office regulations. Female Sprague-Dawley rats (~250 g) were anesthetized, and the left sciatic nerve was exposed and transected at mid-thigh level. The contralateral sciatic nerve was exposed, but not transected. For DRG microinjection, a small laminectomy was performed to expose the left L5 DRG, and 1.5 μl of db-cAMP (dibutyryl cAMP; Sigma) at a concentration of 33 mM in phosphate-buffered saline (PBS) or a similar amount of PBS was injected into the exposed DRG using a Hamilton syringe with a 30-gauge needle. The overlying skin and muscle were sutured, and the animal was allowed to recover.

DRG Cell Line Culture and Transfection—ND7/23 and NDC are hybrid cell lines derived from neonatal rat DRG neurons fused with a mouse neuroblastoma (16). The cell lines were used for some experiments in preference to DRG primary cell cultures (see later) because of the greater ease of transfection. The cells were cultured in Dulbecco's modified Eagle's medium supplemented with 10% fetal bovine serum, 50 units/ml penicillin, 50 μg/ml streptomycin, and 2 mM glutamine at 37 °C in humidified air with 5% CO_2. A Dulbecco's modified Eagle's medium-based medium containing 10% horse serum, 5% fetal bovine serum, penicillin/streptomycin, and glutamine was used to culture PC12 cells. Nerve growth factor (NGF) 7s (100 ng/ml) was added to differentiate PC12 cells.

Two complementary oligonucleotides specific to rat TRPC4 (17) were ordered from Invitrogen. The hairpin RNA oligonucleotides were annealed and ligated into the linearized pSilencer 3.1 H1 hygro vector as described by the manufacturer (Ambion Inc.). The inserts were sequenced to confirm that there were no unwanted mutations. Transfection of ND7/23 was carried out using siPORT XP-1 as directed by the manufacturer's instruction manual (Ambion Inc.). Cells were grown in 6-well plates to 40–60% confluence, and each well was transfected with 1 μg of short hairpin RNA (shRNA) in antibiotic-free medium. Hygromycin (250 μg/ml) was added 24 h after transfection. For mock control, a mismatch hairpin oligonucleotide duplex was inserted into pSilencer 3.1 vector followed by similar transfection. A stable cell line was established in selection medium following the transfection of TRPC4 shRNA or mismatch duplex. Cells were then grown in 125 μg/ml hygromycin for analysis.

Transfection of shRNA-expressing ND7/23 cells with human TRPC4 (hTRPC4, a generous gift from Dr. John Wood) was carried out using Lipofectamine 2000 (Invitrogen) as described by the manufacturer. For each 35-mm Petri dish, hTRPC4 (1 μg) together with enhanced green fluorescent protein (0.3 μg; Clontech) was mixed with diluted lipid reagent for 15 min at room temperature. Cells were incubated with the above complexes for 5 h at 37 °C in humidified air with 5% CO_2. Green fluorescent protein was used as a visual marker for hTRPC4-expressing cells.

To initiate differentiation, the cells were incubated in Dulbecco's modified Eagle's medium containing 0.5% fetal bovine serum and stimulated with 100 ng/ml NGF 7s or 1 mM db-cAMP. Cells were fixed 2 days after differentiation and immunostained for β-tubulin III (1:1000, Sigma), and the length of the longest neurites was measured with ImageJ software. Median lengths and frequency histograms of neurite lengths of 200–350 cells in three bins (<30, 30–100, and >100 μm) were analyzed. The statistical significance was examined using χ^2 analysis.

RT-PCR and Quantitative Real-time PCR—Total RNA was extracted with TRIzol® reagent (Invitrogen) from L4 and L5 DRG of rats subjected to the conditioning or the mock manipulation. Total RNA of DRG cell lines or PC12 cells was prepared similarly. First-strand cDNA was prepared from 1 μg of total RNA with random hexanucleotide primers using Superscript III® reverse transcriptase (Invitrogen). The cDNA was amplified by PCR using TRPC1- and TRPC3–7-specific primers (17). Each amplification reaction contained cDNA derived from 25 ng of RNA, 1.5 mM $MgCl_2$, 400 nM dNTP mix, 200 nM sense and 200 nM antisense primers, and 0.125 μl of *Taq* DNA polymerase (Sigma-Aldrich) in a final volume of 25 μl. Cycling conditions have been described previously (15). An internal control of 18 S ribosomal RNA (18 S rRNA) was performed alongside the experimental samples. PCR products were run and visualized in 2% agarose gel containing ethidium bromide.

Quantitative real-time PCR was performed according to the protocol of the Qiagen QuantiTect™ SYBR® Green PCR kit (Qiagen GmbH, Hilden, Germany) in a Rotor-Gene 3000TM thermocycler (Corbett Research, Sydney, Australia). Melting curves were generated after the last extension step to verify the specificity and identity of PCR products. Each sample was tested in triplicate. The expression level of TRPC transcripts was normalized to the expression of 18 S rRNA and expressed as arbitrary units. When measuring 18 S rRNA, the cDNAs were diluted 200-fold due to its abundance. To compare the expression levels between different TRPC subunits, we calculated the absolute copy numbers of TRPC and 18 S rRNA using standard curves generated with PCR products containing the target sequences. Copy numbers of individual TRPC transcripts were then normalized to those of 18 S rRNA (18).

DRG Neuron Culture and Transfection—DRG neurons were isolated from female Sprague-Dawley rats (~250 g) by methods similar to those described previously (19). Briefly, rats were killed by inhalation of a rising concentration of CO_2 and cervical dislocation. Ganglia from the lumbar level were removed in Ca^{2+}/Mg^{2+}-free Hanks' balanced salt solution. DRG neurons were dissociated by incubation in 0.125% collagenase XI (Sigma) at 37 °C for 2 h. The dispersed cells were suspended, seeded on poly-L-lysine-coated coverslips, and maintained in culture medium containing 0.3% bovine serum albumin, 1% N-2 supplement, and penicillin/streptomycin in Ham's F-12 basal medium (all regents from Invitrogen). After 24 h, neurons were transfected with TRPC4-specific siRNA (sense TACCAAGAGGTGATGAGGATT and antisense 5′-TCCTCATCACCTCTTGGTATT) with a fluorescein label at the 5′-end and mismatch control RNA duplexes (Block-it; Invitrogen) at the final concentration of 50 nM using Oligofectamine (Invitrogen). Cells were then maintained at 37 °C in a humidified atmosphere of 95% air and 5% CO_2.

TRPC4 sense (5′-GAAGATGGTGACATGTTTCATAATAG), antisense (5′-CTATTATGAAACATGTCACCATCTTC), and scrambled control oligonucleotides containing modified T-phosphorothioate bases were ordered from Invitrogen (20). A 5′-fluorescein was added to the primers

when monitoring the transfection efficiency or examining the possible functional role of TRPC4 in DRG neurons. Freshly dissociated DRG neurons were mixed with oligonucleotide-Oligofectamine (Invitrogen) complexes on ice for 30 min before being plated on poly-L-lysine-coated coverslips. The final concentration of each oligonucleotide was 100 nM. Neurons were analyzed 48 h after transfection.

To quantify the length of neurites, DRG neurons were fixed 2 days after transfection and immunostained for β-tubulin III (1:1000, Sigma), and the length of the longest neurites of each cell was measured with ImageJ software. Previous studies indicate that a subpopulation of DRG neurons identified by *Griffonia simplicifolia* isolectin B4 give rise to little neurite outgrowth in normal culture conditions (21). Therefore, we excluded those cells whose longest neurites failed to reach twice the length of the cell bodies. Median lengths and frequency histograms of neurite lengths of ~100 cells were analyzed.

Immunohistochemistry—Sprague-Dawley rats were anesthetized with an intraperitoneal injection of sodium pentobarbital (60 mg/kg; Sagatal) and then perfused with 0.9% saline followed by 4% paraformaldehyde in 0.1 M phosphate buffer at 12 h, 3 days, or 7 days after left sciatic nerve axotomy. Two rats were used for each time point, and two rats without sciatic nerve lesion were used as control. Cultured DRG neurons and ND7/23 cells were fixed in 4% paraformaldehyde, pH 7.4, for 15 min at room temperature. TRPC4 staining was visualized using the tyramide signal amplification technique. Briefly, sections were labeled with a rabbit polyclonal antibody against TRPC4 (1:1000; Alomone) overnight followed by incubation in donkey anti-rabbit biotin (1:400) for 90 min. Sections were then incubated in avidin-biotin peroxidase complex from an ABC kit (Vector Laboratories) for 60 min, followed by incubation in cyanine 3 tyramide solution (1:75; PerkinElmer Life Sciences) for 7 min. TRPC4 peptide antigen was added to control slides to test the specificity of the primary antibody.

Slides were also stained with mouse anti-200-kDa neurofilament (N52 clone, 1:5000; Sigma) and rabbit anti-$P2X_3$ (1:1000; Neuromics) or rabbit anti-CGRP (1:1000) antibodies to visualize distinct DRG subpopulations. Fluorescein isothiocyanate-conjugated goat anti-rabbit Ig G (1:400; Jackson Laboratories) and 7-amino-3-methyl-coumarin acetic acid-conjugated goat anti-mouse Ig G (1:400; Jackson Laboratories) were added for 2 h following rinses with PBS. All slides were pre-blocked in 10% normal donkey serum containing 0.2% Triton X-100 for 1 h. Primary antibodies were diluted in PBS containing 0.2% Triton X-100 and 0.1% sodium azide. Sections were viewed on a Leica epifluorescence microscope (Wetzlar, Germany), and micrographs were taken at ×20 objective magnification. The total number of neurons per section was counted based on Hoechst labeling. Neurons showing TRPC4 immunoreactivity were counted and expressed as a percentage of total DRG neurons or a percentage of a subpopulation such as N52- positive or $P2X_3$-positive neurons. One-way analysis of variance was used to compare the numbers of TRPC4-positive cells from 0 to 3 days after nerve injury. For total DRG or TRPC4-immunoreactive cell size distribution, 250 DRG neurons were measured on randomly chosen sections using ImageJ software.

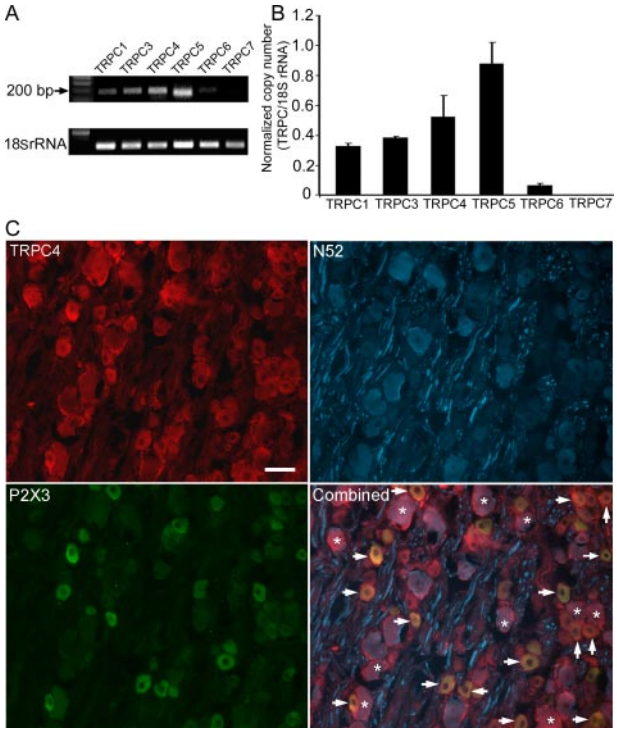

FIGURE 1. **TRPC channels are present in adult DRG neurons.** *A*, RT-PCR products of mRNA isolated from adult rat DRG are shown using primers for TRPC1, TRPC3-TRPC7, and 18 S rRNA. *B*, relative levels of different TRPC transcripts determined by quantitative real-time PCR and expressed as absolute copy numbers normalized to those of 18 S rRNA mean ± S.E. *C*, immunohistochemical staining of TRPC4, N52, and $P2X_3$ in rat DRG cryosections. Neurons double-labeled with TRPC4 and N52 are indicated by an *asterisk*, and those with TRPC4 and $P2X_3$ by an *arrow* in the combined image. *Scale bar*, 50 μm.

Confocal Microscopy—DRG neurons or cell lines with TRPC4 labeling were examined using an upright Zeiss confocal laser scanning microscope system (LSM 510) and a ×63 Plan Neofluor oil objective. Cells were scanned for cyanine 3 at 543 nm with an increment of 0.25 μm in the Z plane.

Immunoblotting—Sprague-Dawley rats were sacrificed at 4, 7, or 14 days after left sciatic nerve axotomy. Two rats were used for each time point, and two rats without sciatic nerve lesion were used as control. The left L4 and L5 DRG were collected, cut into pieces using fine scissors, and homogenized in 200 μl of lysis buffer containing protease inhibitors (Roche Applied Science). For cell line preparations, cells were washed in cold PBS, pelleted, and resuspended in radioimmune precipitation lysis buffer containing protease inhibitors. Samples were then solubilized by rotation at 4 °C for overnight. The lysate was centrifuged at 13,000 × *g* for 15 min, and the supernatant was collected. Protein concentration was measured using the DC protein assay (Bio-Rad), and the lysates were subjected to electrophoresis on 6.5% SDS-PAGE gels, transferred onto polyvinylidene difluoride membrane, and blotted with polyclonal rabbit TRPC4 antibody (1:100; Alomone) overnight at 4 °C. Anti-rabbit immunoglobulin horseradish-linked secondary antibody (Amersham Biosciences) was used at a final dilution of 1:5000, and the signal was detected with the ECL Plus Western blotting detection system. The membranes were subsequently stripped and re-blotted with mouse anti-actin antibody (1:500; Sigma). Protein levels of TRPC4 were determined using ImageJ software and were normalized to corresponding actin levels.

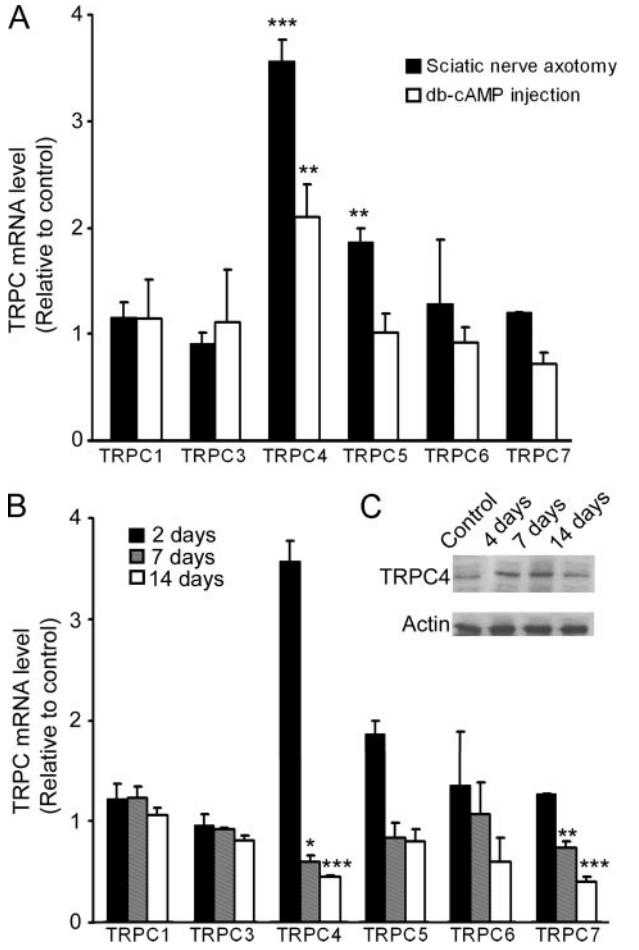

FIGURE 2. **TRPC4 is transiently up-regulated during regenerative conditions.** *A*, TRPC mRNA levels in L4 and L5 DRG at day 2 following either left sciatic nerve injury or intra-ganglionic microinjection of db-cAMP. Transcript levels of TRPC subunits from rats with nerve injury were expressed in relation to that of mock axotomy, and the latter was designated as 1. TRPC levels in db-cAMP-injected DRG were expressed in relation to that of PBS-injected DRG. *B*, TRPC transcript levels at days 7 and 14 after sciatic nerve axotomy. Data of TRPC levels at postoperative day 2 are shown for comparison. Mean ± S.E.; ***, $p < 0.001$; **, $p < 0.01$; *, $p < 0.05$ compared with control (*A*) and compared with 2 days (*B*), unpaired Student's *t* test. *C*, Western blotting analysis for TRPC4 and actin at days 4, 7, and 14 after nerve injury.

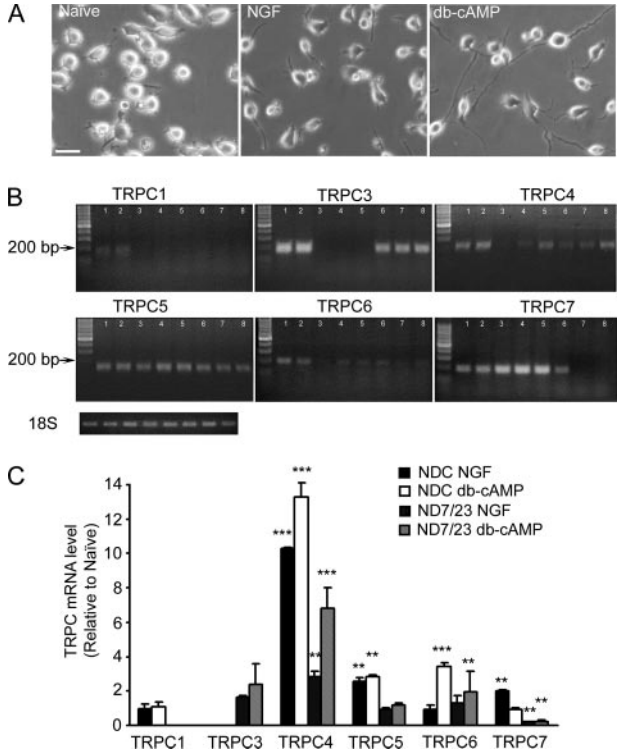

FIGURE 3. **Changes in TRPC transcript levels during the differentiation of NDC and ND7/23 cells.** *A*, phase-contrast micrograph of naïve and differentiated ND7/23 cells treated with NGF and db-cAMP. *Scale bar*, 50 μm. *B*, transcript levels of TRPC subunits in naïve and differentiated PC12, NDC, and ND7/23 cells. *Lanes 1–2* show RT-PCR products of naïve and NGF-treated PC12 cells; *lanes 3–5* show those of naïve, NGF-, and db-cAMP-treated NDC cells; *lanes 6–8* show those of naïve, NGF-, and db-cAMP-treated ND7/23 cells. 18 S rRNA is shown as the loading control. *C*, changes in TRPC subunits in differentiated NDC and ND7/23 cells determined by quantitative RT-PCR. mRNA levels of TRPC channels in differentiated cells were normalized to those in naïve cells and the latter was designated as 1 (mean ± S.E.; ***, $p < 0.001$; **, $p < 0.01$, Student's *t* test).

RESULTS

TRPC Channels Are Present in Adult Rat Sensory Neurons—First, we used specific primers for rat TRPC1 and TRPC3-TRPC7 to determine whether DRG neurons express TRPC channels. Our RT-PCR analysis showed that variable levels of TRPC1, TRPC3, TRPC4, TRPC5, and TRPC6 were expressed in dorsal root ganglia (Fig. 1*A*). TRPC7 was not detected in three separate tests. Quantitative real-time PCR assays were performed using SYBR® Green, and absolute copy numbers of various TRPC channels were calculated. We found that TRPC4 and TRPC5 appeared to be most abundant, followed by TRPC1 and TRPC3. TRPC6 and TRPC7 mRNAs were at much lower concentrations (Fig. 1*B*).

Next, we examined TRPC4 protein expression in adult rat ganglia using immunohistochemical labeling. TRPC4 immunoreactivity was detected in ~55% of total DRG neurons as identified by Hoechst staining. Schwann cells and satellite cells were weakly labeled with TRPC4. Staining with N52 and $P2X_3$ or CGRP was used to label large and small neurons associated with myelinated or unmyelinated fibers. Fig. 1*C* shows representative images of DRG cryosections triple labeled with TRPC4, N52, and $P2X_3$. The combined image shows TRPC4 immunoreactivity in different DRG subpopulations. Quantitative analysis showed that 38 ± 3% ($n = 316$) of N52-positive neurons were TRPC4-immunoreactive and 75 ± 6% ($n = 300$) of $P2X_3$-positive neurons were TRPC4-immunoreactive. Approximately 69 ± 5% ($n = 258$) of CGRP-positive neurons were TRPC4-positive.

TRPC4 Transcript Is Increased Following Nerve Injury and db-cAMP Injection—We have previously reported that both sciatic nerve axotomy and db-cAMP microinjection accelerate axonal regeneration after crush injury of the corresponding dorsal spinal nerve root (15). Here we found that the transcript levels of TRPC4 and TRPC5 were increased to 357 ± 20% ($n = 3$, $p < 0.001$) and 186 ± 14% ($p < 0.01$, $n = 3$) 2 days after nerve injury. Microinjection of db-cAMP up-regulated TRPC4 to 223 ± 35%, ($p < 0.01$, $n = 3$) but had no effect on TRPC5 (107 ± 21%, $p > 0.05$, $n = 3$). TRPC1, TRPC3, TRPC6, and TRPC7 were not markedly altered following sciatic nerve transection or db-cAMP injection (Fig. 2*A*).

Next, we examined transcript levels of TRPC subunits at days 7 and 14 after a priming lesion in the left sciatic nerve (Fig. 2*B*). The concentration of TRPC4 transcript peaked at 2 days and

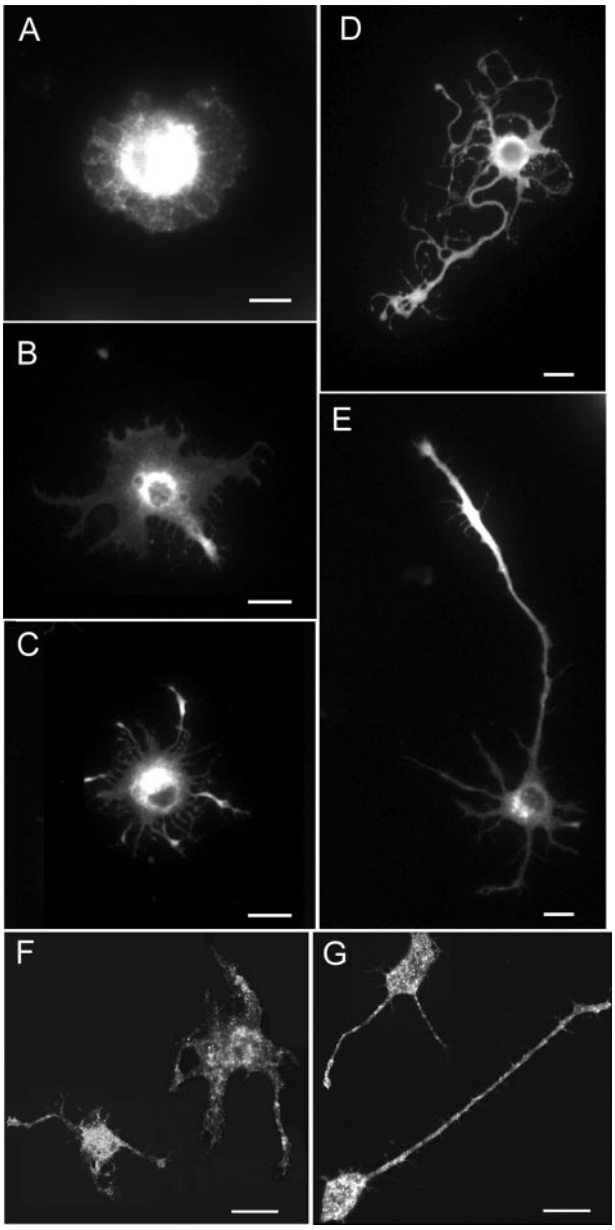

FIGURE 4. **TRPC4 is present in the growth cone in adult sensory neurons.** Representative confocal microscopic images show outgrowth of neurites at various stages: membranous expansion (*A*), neurite formation (*B*, *C*), and elongation (*D*, *E*). TRPC4 immunoreactivity was found in the cell membrane, in the cytosol, along the neurite process, and in the growth cone of DRG neurons. Naïve (*F*) and differentiated (*G*) ND7/23 cells were also immunoreactive for TRPC4. *Scale bars*, 20 μm.

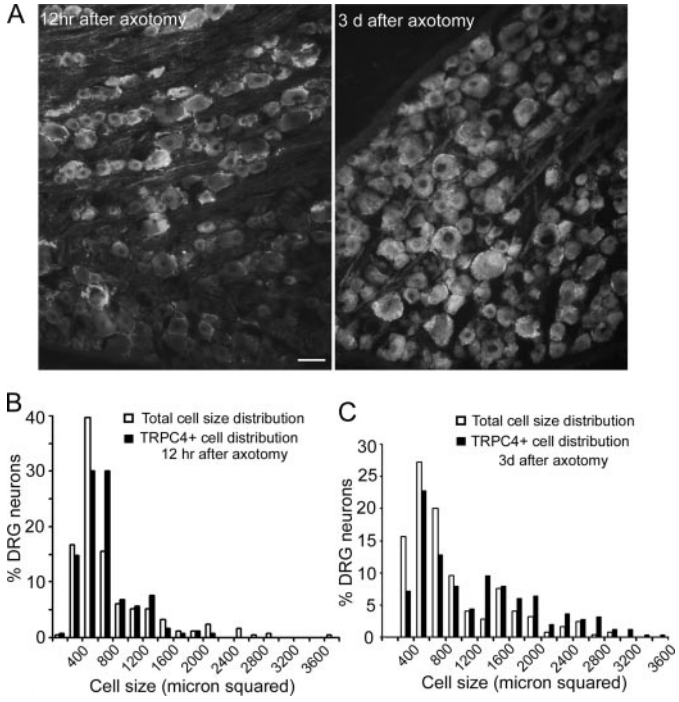

FIGURE 5. **Nerve injury increases the proportion of TRPC4-immunoreactive DRG neurons.** *A*, TRPC4 staining 12 h and 3 days after sciatic nerve injury. *Scale bar*, 50 μm. *B* and *C*, histograms of total DRG cell size distribution and the cell size distribution of TRPC4-immunoreactive cells at 12 h and 3 days after sciatic nerve transection.

fell to 56 ± 5% ($n = 3$, $p < 0.05$) and 43 ± 1% ($n = 3$, $p < 0.001$) at 7 and 14 days. TRPC5 mRNA was halved at 7 days (79 ± 14%, $n = 3$, $p > 0.05$) when compared with that of 2 days but was not further reduced at 14 days (76 ± 11%, $n = 3$, $p > 0.05$). Transcripts of TRPC1, TRPC3, and TRPC6 were not significantly changed from 2 to 7 days after nerve injury. However, TRPC7 mRNA levels were reduced to 70 ± 5% ($n = 3$, $p < 0.01$) at 7 days and 38 ± 4% ($n = 3$, $p < 0.001$) at 14 days. Thus, nerve injury elicited a transient increase in TRPC4 and a significant reduction in TRPC7.

TRPC4 protein was analyzed in L4 and L5 DRG at days 4, 7, and 14 following nerve injury. A single band specific for TRPC4 was detected by rabbit anti-TRPC4 polyclonal antibody (Fig. 2*C*). TRPC4 protein levels were expressed in relation to the loading control of actin using ImageJ analysis. TRPC4 protein was increased by 2.1- and 3-fold at 4 and 7 days and reduced to control level at day 14 after nerve injury.

TRPC4 mRNA Is Substantially Increased in Differentiated NDC and ND7/23 Cells—Fig. 3*A* shows naïve and differentiated ND7/23 cells visualized under phase-contrast illumination. Naïve ND7/23 cells gave rise to short neurites 2 days after plating. In the presence of NGF (100 ng/ml) or db-cAMP (1 mM), cells stopped proliferating and generated long unbranched neurites. RT-PCR analyses were carried out on naïve and differentiated NDC and ND7/23 cells and in naïve and differentiated PC12 cells. Fig. 3*B* shows representative results from one of three similar experiments. Transcripts for TRPC1, TRPC4, and TRPC5–7 were found in naïve and differentiated NCD cells, whereas transcripts for TRPC3–7 were found in naïve and differentiated ND7/23 cells. A discernible increase in TRPC4 mRNA was observed in differentiated NDC and ND7/23 cells, and a marked reduction in TRPC7 mRNA was observed in differentiated ND7/23 cells. In contrast, transcripts of TRPC1 and TRPC3–7 were found in both naïve and differentiated PC12 cells and no discernible changes were observed.

We further quantified changes in TRPC1 and TRPC3–7 transcripts in naïve and differentiated NDC and ND7/23 cells using SYBR Green (Fig. 3*C*). TRPC4 transcript was increased by ~10- and 13-fold in NDC cells after stimulation with NGF or db-cAMP for 2 days. An increase in TRPC4 mRNA of ~3- and 7-fold was observed in differentiated ND7/23 cells. TRPC1 was not detected in ND7/23 cells and not markedly changed in

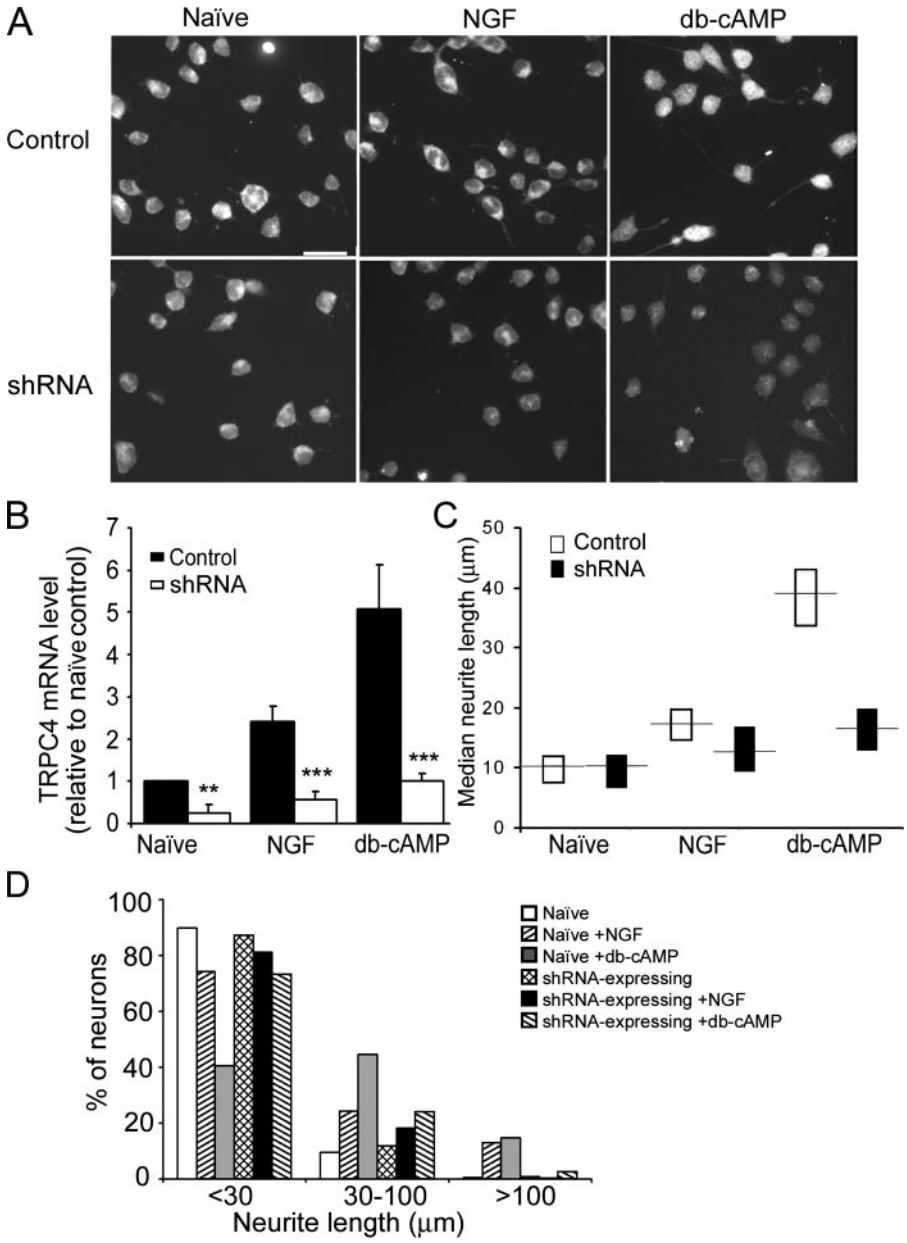

FIGURE 6. **Down-regulation of TRPC4 using specific shRNA impairs neurite outgrowth in ND7/23 cells.** *A*, TRPC4 staining in control (scrambled shRNA) and shRNA-expressing ND7/23 cells in the presence and absence of NFG or db-cAMP. shRNA-expressing cells showed weak TRPC4 immunoreactivity and bore short neurites. *Scale bar*, 50 μm. *B*, real-time RT-PCR analysis of TRPC4 in control and shRNA-expressing cells in naïve, NGF, or db-cAMP-treated cells. shRNA reduces the concentrations of TRPC4 mRNA in comparison to that of naïve ND7/23 cells in the absence or presence of NGF/db-cAMP (mean ± S.E.; ***, $p < 0.001$; **, $p < 0.01$, Student's *t* test). *C*, summary of median lengths and 95% confidence levels in control and shRNA-expressing cells in the absence and presence of NGF or db-cAMP. In NGF- or db-cAMP-treated cultures, shRNA reduces median neurite length compared with controls. *D*, frequency histogram showing the percentage of cells with neurites in each of the three length ranges ($n = 200–350$). In the presence of NGF or db-cAMP, the distribution of neurite lengths for control cells differs significantly from that for shRNA-expressing cells by χ^2 analysis ($p < 0.01$ and $p < 0.001$, respectively).

NDC cells. TRPC3 was not detected in NDC cells and moderately increased in ND7/23 cells stimulated with NGF (1.6-fold) or db-cAMP (2.4-fold). A 3-fold increase in TRPC5 mRNA was observed in differentiated NDC cells, but no marked increase was observed in ND7/23 cells. db-cAMP increased the TRPC6 mRNA level by 3.5-fold in NDC cells and 2-fold in ND7/23 cells, whereas NGF did not markedly alter TRPC6 transcript in NDC and ND7/23 cells. A moderate increase of 2-fold was observed in TRPC7 mRNA in NDC cells treated with NGF, but not with db-cAMP. However, NGF and db-cAMP reduced the level of TRPC7 mRNA by ~80% in ND7/23 cells.

TRPC4 Is Present in the Growth Cone of Cultured DRG Neurons—To examine TRPC4 expression during different stages of neurite outgrowth, we fixed DRG neurons at 6, 12, 24, and 48 h after plating. Fig. 4 shows confocal microscopic images of outgrowth of neurites at various stages from membrane expansion (Fig. 4*A*), neurite formation (Fig. 4, *B* and *C*), and neurite elongation (Fig. 4, *D* and *E*). The neurite process started as a membranous expansion around the soma, evolving into the extension of small sprouts from the membranous expansion and finally elongation into filopodia. Subsequently, some neurites were selected for extension by a mechanism that is not fully understood. We found that membranous expansions and filopodia were positively stained for TRPC4. Longer neurites appeared to be more intensely labeled with TRPC4 than shorter neurites of the same neurons (Fig. 4, *D* and *E*), an observation suggesting that TRPC4 was selectively enriched in elongating neurites. TRPC4 immunoreactivity was also found in all naïve and differentiated ND7/23 cells stimulated with db-cAMP (Fig. 4, *F* and *G*). TRPC4 staining as irregular punctae was present in the cell membrane, in the cytosol, along the neuronal process, and in finger-like projections characteristic of growth cones.

Nerve Injury Increases TRPC4-immunoreactive DRG Neurons—Immunostaining of tissue sections was carried out to determine whether the increased TRPC4 expression observed in DRG after nerve injury occurs in neurons or glia. TRPC4 immunoreactivity increased from ~50% of DRG neurons to 70% from 12 h to 3 days after sciatic nerve axotomy ($p < 0.01$, Fig. 5*A*). Schwann cells weakly express TRPC4; however, the increase in the percentage of TRPC4-positive Schwann cells was negligible (24 *versus* 25%). To investigate in which subpopulations of DRG neurons TRPC4 immunoreactivity was increased, we compared the total cell size distribution and TRPC4-positive cell

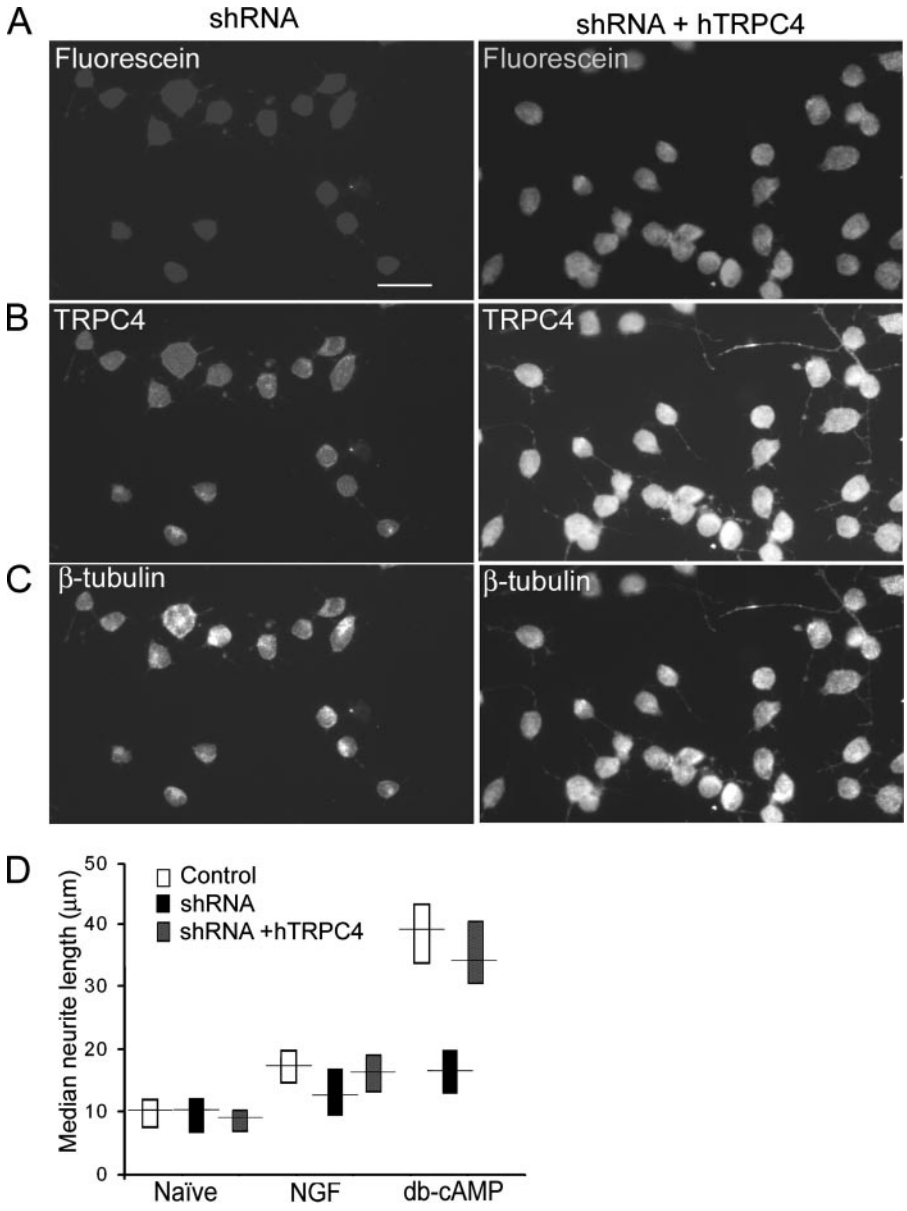

FIGURE 7. **Overexpression of hTRPC4 rescues neurites from the shortening induced by shRNA expression in ND7/23 cells.** *A* and *B*, hTRPC4/shRNA-expressing cells are green fluorescent protein-positive and show high density of TRPC4 immunoreactivity. In contrast, shRNA-expressing cells showed either no or weak TRPC4 labeling. *C*, hTRPC4/shRNA-expressing cells grew longer neurites than shRNA-expressing cells after db-cAMP incubation for 48 h. The length of neurites was measured with β-tubulin staining as a visual marker. *Scale bar*, 50 μm. *D*, summary of median lengths and 95% confidence levels in shRNA-expressing and hTRPC4/shRNA cells in the absence and presence of NGF or db-cAMP.

size distribution at 1 and 2 h and 3 days after nerve transection (Fig. 5, *B* and *C*). Previous studies indicate that cells larger than 1000 μm^2 in area correspond to cells with myelinated axons and Aα/β conduction velocities (22). Thus, we adopted 1000 μm^2 as a cutoff point to distinguish small and large sized neurons. It appears that nerve injury shifted the distribution of TRPC4-positive cells toward large sized neurons. Approximately half of TRPC4-positive neurons (49.2%) were in the category of large cells at 3 days postoperatively compared with about a quarter of TRPC4-positive neurons (24.4%) at 12 h. Changes in the TRPC4 expression profile in DRG subpopulations were confirmed when we triple labeled DRG sections for TRPC4, N52, and $P2X_3$/CGRP immunoreactivity. Three days after sciatic nerve injury, ~63% of large myelinated neurons indicated by N52 staining ($n = 134$) were TRPC4-immunoreactive-positive. Of small unmyelinated neurons identified by $P2X_3$ or CGRP staining, ~81 or 86%, respectively, were TRPC4-immunoreactive.

Suppression of TRPC4 mRNA Inhibits the Elongation of Neurites in ND7/23 Cells—Fig. 6*A* shows TRPC4 staining in naïve and differentiated ND7/23 cells expressing either a scrambled sequence (*Control*) or TRPC4-specific shRNA. shRNA-expressing cells showed discernible weak TRPC4 immunoreactivity in three separate preparations. Using a previously identified shRNA specifically targeting TRPC4 (17), we were able to suppress TRPC4 mRNA by 74% measured by real-time PCR (Fig. 6*B*). The control shRNA with scrambled sequence had no effect on TRPC4 expression. TRPC4 transcript levels were normalized to that of control cells in the absence of NGF or db-cAMP. In the presence of NGF or db-cAMP, TRPC4 mRNA in shRNA-expressing cells was ~23 and 20% when compared with that of control cells. The length of neurites was markedly reduced in shRNA-expressing cells. In control ND7/23 cells, median neurite lengths in the presence of NGF or db-cAMP were 17.4 and 39.1 μm, as compared with 9.5 μm in undifferentiated cells. In shRNA-expressing cells, median neurite lengths in the presence of NGF or db-cAMP were 12.7 and 16.5 μm, as compared with 10.4 μm in the unstimulated condition (Fig. 6*C*). The distribution of neurite lengths for control and shRNA-expressing cells in the absence of NGF or db-cAMP was not significantly different by the χ^2 test. In contrast, distribution of neurite lengths for control cells stimulated by NGF or db-cAMP differed with high significance from that for shRNA-expressing cells ($p < 0.01$).

Overexpression of Human TRPC4 Rescues Neurite Shortening in shRNA-expressing Cells—The sequence of human TRPC4 (hTRPC4) contains a 2-nucleotide mismatch when compared with that of shRNA targeting rat TRPC4. We examined whether overexpression of hTRPC4 could rescue neurite shortening in shRNA-expressing ND7/23 cells. Transfection efficiency of hTRPC4 was ~80% as estimated by green fluorescent protein expression (Fig. 7*A*). We found that almost all green

fluorescent protein-positive cells in three separate preparations were labeled with TRPC4 immunoreactivity (Fig. 7, *A* and *B*). In contrast, shRNA-expressing cells displayed either no or weak TRPC4 staining. Following the incubation with NGF or db-cAMP for 48 h, the length of neurites in shRNA-expressing cells and TRPC4/shRNA-expressing cells was measured after β-tubulin staining (Fig. 7*C*). In the presence of NGF or db-cAMP, overexpression of hTRPC4 increased the median neurite length from 12.7 and 16.5 μm to 16.2 and 34.2 μm (Fig. 7*D*). Distribution of neurite lengths for hTRPC4/shRNA-expressing cells significantly differed from that for shRNA-expressing cells upon differentiation with db-cAMP ($p < 0.001$, χ^2 test). The median lengths of control ND7/23 cells in the presence of NGF or db-cAMP were 17.4 and 39.1 μm. Thus, it appeared that overexpression of hTRPC4 reversed, at least partially, the impairment of neurite elongation caused by shRNA expression.

Inhibition of TRPC4 Impairs Neurite Outgrowth in DRG Neurons—Fluorescein-labeled TRPC4 siRNA and scrambled RNA duplex were tested in cultured DRG neurons. A transfection rate of 60% was routinely achieved (Fig. 8*A*), and transfection had no effects on cell survival during 2 days determined by trypan blue staining. The efficacy of TRPC4-specific siRNA was validated with Western blotting analysis (Fig. 8*B*). Levels of TRPC4 protein in DRG transfected with scrambled or siRNA were expressed in relation to the loading control of actin and were normalized to the level of the control preparation. TRPC4-specific siRNA repressed TRPC4 expression to 23.6 ± 1% of controls ($n = 3$, $p < 0.01$, Student *t* test), whereas the scrambled RNA duplexes had no significant effect on TRPC4 expression (Fig. 8*C*). We found that the elongation of neurites was markedly impaired in neurons transfected with TRPC4-specific siRNA (Fig. 8*D*). The median neurite length in DRG neurons transfected with TRPC4-specific siRNA was 116.9 μm (with a 95% confidence range of 97.5 to 136.0 μm, $n = 92$), whereas that in control preparations was 234.9 μm (with 95% confidence range of 223.6 to 270.3 μm, $n = 96$, Fig. 8*E*). The distribution of neurite lengths for control and scrambled siRNA preparations was not significantly different by the χ^2 test. In contrast, distribution of neurite lengths for DRG transfected with TRPC4-sepcific siRNA differed with high significance from that of control cells (Fig. 8*F*, $p < 0.001$, χ^2 test).

A recent publication showed that the growth and maintenance of synapses and dendritic spines were sensitive to off-target effects of siRNA (23). To corroborate our findings from siRNA experiments, we employed a previously identified antisense to knock down TRPC4 expression in DRG neurons (20). 5′-fluorescein was used as a marker for oligonucleotide-positive neurons. We found that transfection efficiency for oligonucleotide primers was ~80% in DRG cells (Fig. 9, *A* and *B*). Using antisense specifically targeting TRPC4, we were able to suppress TRPC4 mRNA by 89% measured by real-time PCR (Fig. 9*C*). Sense and scrambled oligonucleotides had no significant effect on the level of TRPC4 transcript expressed as percentage of that of control neurons after normalization to the corresponding level of 18 s rRNA. The median neurite length in DRG neurons transfected with TRPC4 antisense was 125.2 μm with a 95% confidence range of 98.4 to 136.9 μm ($n = 86$), as compared with 240.8 μm in control DRG preparations with a 95% confidence range of 215.6 to 274.8 μm ($n = 71$).

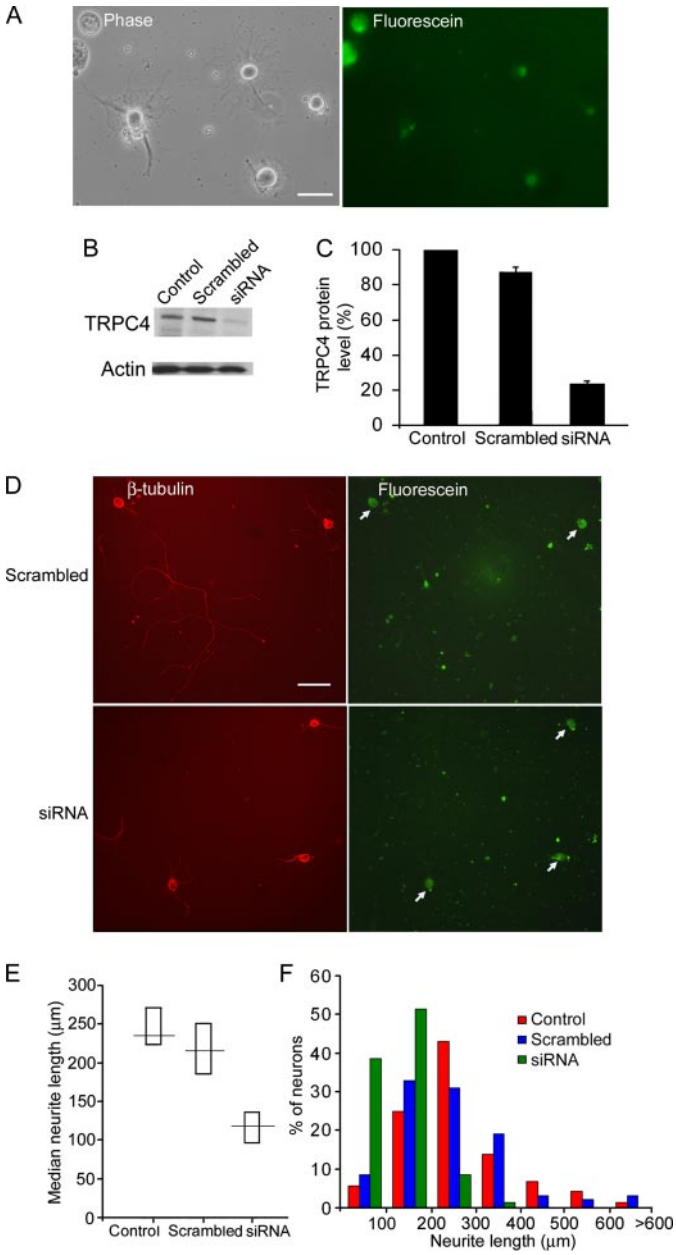

FIGURE 8. **TRPC4 contributes to neurite elongation in cultured DRG neurons.** *A*, dissociated rat DRG neurons transfected with TRPC4-specific siRNA. Transfected cells are visible in the fluorescein image. *Scale bar*, 50 μm. *B*, Western blotting analysis of TRPC4 and actin (internal loading control) 48 h after transfection. Each lane was loaded with ~90 μg of protein determined by DC protein assay. *C*, quantitative analysis of TRPC4 protein in DRG transfected with scrambled and specific TRPC4 siRNA in relation to the corresponding actin levels mean ± S.E. siRNA-treated cells show markedly reduced TRPC4 expression. *D*, β-tubulin III-labeled DRG neurons transfected (*arrows*) with scrambled or TRPC4 siRNA. siRNA-transfected cells show greatly reduced neurites compared with scrambled controls. *Scale bar*, 100 μm. *E*, median lengths and the 95% confidence ranges of the longest neurites in cultured sensory neurons transfected with scrambled or TRPC4 siRNA. siRNA-transfected cells show greatly reduced median neurite length compared with controls. *F*, frequency histogram showing the percentage of cells with neurites in each of the seven length ranges ($n = ~100$). The distribution of neurite lengths for cells transfected with TRPC4 siRNA differs significantly from that for cells transfected with scrambled RNA duplexes ($p < 0.001$, χ^2 analysis).

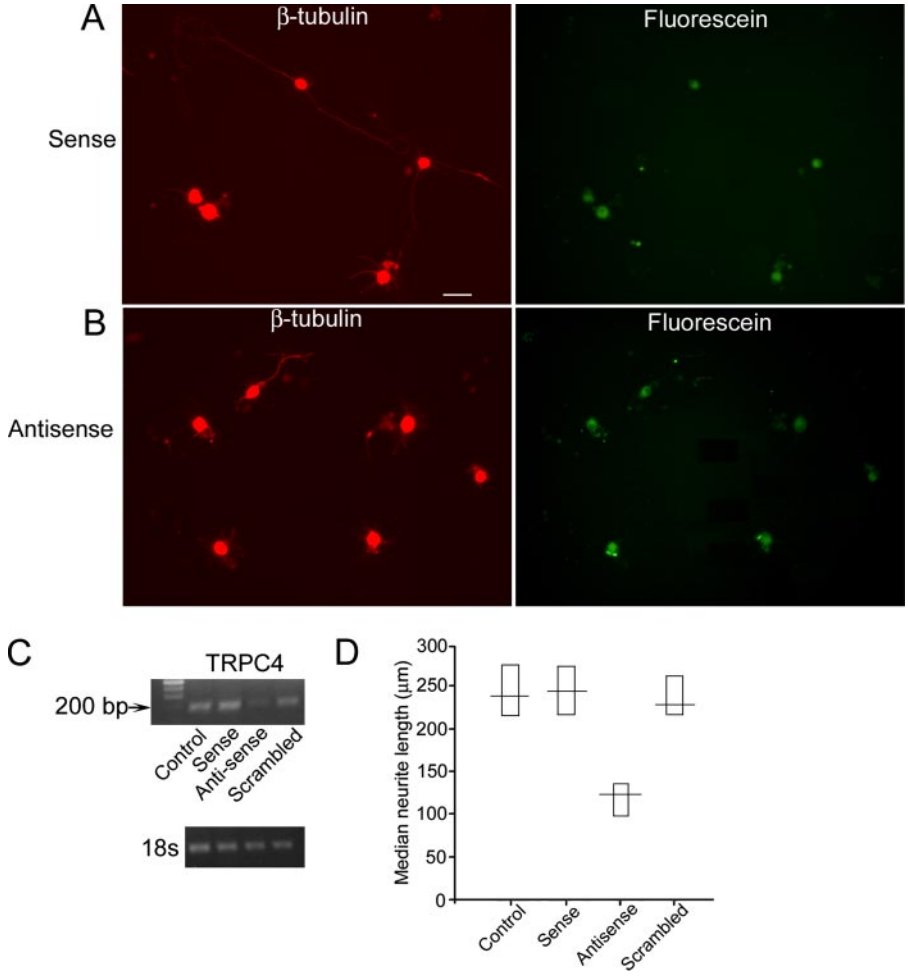

FIGURE 9. **Knock down of TRPC4 expression using antisense reduces the neurite length in cultured DRG neurons.** *A* and *B*, TRPC4-specific antisense, but not sense, reduces the neurite elongation in DRG cells. Both antisense and sense were tagged with 5′-fluorescein. *Scale bar*, 50 μm. *C*, the transcript level of TRPC4 in control DRG cells and those transfected with sense, antisense, or scrambled oligonucleotides. 18 S mRNA were used as a loading control. *D*, median lengths and the 95% confidence ranges of the longest neurites in control sensory neurons and those transfected with sense, antisense, or scrambled oligonucleotides. Cells transfected with antisense show reduced median neurite length in comparison to controls.

DISCUSSION

Several lines of evidence indicate a potential functional role of TRPC4 in axonal regeneration. TRPC4 transcript and protein are increased in the DRG after sciatic nerve transection. By immunohistochemistry, at least some of the increased TRPC4 is found in neurons, particularly large sized ones. In cultured sensory neurons, TRPC4 is present along the process of neurites and in growth cones. Most directly, suppression of TRPC4 synthesis by specific siRNA or antisense halves the median length of neurites in DRG neurons. Thus, the temporal and spatial distributions of TRPC4 in injured neurons, together with the functional data, strongly suggest that TRPC4 contributes to axonal regeneration in primary sensory neurons after injury.

Microarray studies have revealed that over 200 genes, including those coding for ion channels, G protein-coupled receptors, cytokines/growth factors, cell cytoskeleton, and transcription factors are altered in injured DRG neurons (24–26). Here, we report that TRPC channels are present in mammalian sensory neurons and that TRPC4 is increased after nerve injury. Genes that have been identified in array studies show a diverse pattern over time, probably reflecting their different functions in fast adaptive response, survival, regeneration, or neuropathic pain. In addition to TRPC4, other molecules such as interleukin-6 (IL-6) and heat shock protein 27 (Hsp27) undergo a transient increase after nerve injury (24, 25, 27). For example, IL-6, which is undetectable after development, reappears within 1 day, maximally increases between 2 and 4 days, and decreases below the detection threshold within 7 days after nerve injury (27). The beneficial effect of IL-6 is thought to be due to the induction of BDNF in injured sensory neurons, and the role of Hsp27 on various stages of neurite outgrowth is probably due to the modulation of actin cytoskeletal dynamics (28, 29). TRPC4 induction is likely to have a function related to other proteins in DRG neurons that are increased over the same time course.

TRPC receptors are Ca^{2+}-permeable cation channels that are activated downstream of phospholipase C β or phospholipase C γ following stimulation of G protein-coupled receptors or receptor tyrosine kinases. The precise mechanisms by which TRPC4 is activated are not fully understood. Recent studies have shed light on the mechanisms underlying the activation of TRPC channels by growth factors. For example, TRPC3 is activated by BDNF via a phospholipase C γ- inositol 1,4,5-trisphosphate receptor pathway in central nervous system neurons (9). TRPC5 is present in neuronal cytoplasmic transport vesicles, and its activation is controlled by epidermal growth factor and BDNF through control of rapid vesicular translocation and insertion (30, 31). BDNF synthesis and anterograde transport are increased in large diameter DRG neurons within 24 h after sciatic nerve injury (24, 25, 32, 33). Thus, it is likely that TRPC4 activity in growth cones is enhanced by an increased release of growth factors after nerve injury.

In the nerve cell body, elevation of intracellular Ca^{2+} following TRPC4 activation might regulate numerous physiological processes through a wide range of target proteins such as cAMP response element-binding protein and mitogen-activated protein kinase/extracellular-regulated kinase that in turn regulate gene expression (34, 35). Beneficial effects of TRPC4 on the neurite outgrowth might also be exerted through Rho GTPases, a family of small GTP-binding proteins encompassing Rho,

Rac, and Cdc42 subfamilies. Recent studies have revealed a close relationship between TRPC channels and the activation of RhoA (36, 37). For example, TRPC6-mediated Ca^{2+} influx induces RhoA activation and results in endothelial cell contraction (37). In the growth cone, Ca^{2+} also plays a key role in regulating cytoskeletal molecules and membrane dynamics via various signaling molecules such as the growth-associated protein GAP43 (2, 38, 39). Previous studies have shown that GAP43-like proteins promote neurite outgrowth, anatomical plasticity, and nerve regeneration by modulating phosphatidylinositol 4,5-bisphosphate at plasmalemmal rafts (40). GAP43-like proteins contain a basic domain that binds calcium/calmodulin, actin filaments, protein kinase C, and phosphatidylinositol 4,5-bisphosphate (41). Ca^{2+} entering the cytoplasm upon the activation of the TRPC4 channel could bind calmodulin and interact with the basic domain of GAP43, which could result in actin cytoskeleton remodeling. Further studies are required to examine the downstream signaling pathways of TRPC4 and to understand the mechanism by which TRPC4 enhances neurite outgrowth.

Our results have shown that suppression of TRPC4 through shRNA, siRNA, and antisense reduces the length of neurites in ND7/23 cells and adult DRG neurons. The specificity of this suppression was established using appropriate scrambled or sense controls and by showing that the overexpression of hTRPC4 overcomes the suppression due to shRNA (23). Interestingly, previous studies show that dominant-negative TRPC5 expression promotes neurite outgrowth and filopodia formation in hippocampal neurons (30, 31). These data indicate that the functions of TRPC channels depend on the specific assembly of TRPC subunits, the tissue type, and the age of animals. TRPC expression in various cell types typically is not limited to a single member but a combination of various TRPC subunits (18, 42–44). In addition, the TRPC expression profile changes during development. For example, TRPC4 is significantly reduced during postnatal development of the cerebellum (45). It has been found that the TRPC4 subunits can form heteromeric channels within a given structural subfamily, such as with TRPC5, and beyond the structural subfamily, as with TRPC1 and TRPC3 (46–49). Thus, reduction of TRPC4 expression by specific shRNA or siRNA might affect the function of both TRPC4 homomers and TRPC4-containing heteromers and the impairment of neurite elongation might be an overall consequence of the reduction of more than one assembly.

Our data strongly suggest an important role of TRPC4 in sensory axonal regeneration and establish TRPC4 as a potential therapeutic target for promoting regeneration after nerve injury.

Acknowledgments—We thank Dr. John Wood for providing ND7/23 and NDC cell lines. We thank Dr. Xuenong Bo for useful discussions and Dr. Xinyu Zhang for excellent technical help.

REFERENCES

1. Henley, J., and Poo, M. M. (2004) *Trends Cell Biol.* **14,** 320–330
2. Gomez, T. M., and Zheng, J. Q. (2006) *Nat. Rev. Neurosci.* **7,** 115–125
3. Shim, S., Goh, E. L., Ge, S., Sailor, K., Yuan, J. P., Roderick, H. L., Bootman, M. D., Worley, P. F., Song, H., and Ming, G. L. (2005) *Nat. Neurosci.* **8,** 730–735
4. Wang, G. X., and Poo, M. M. (2005) *Nature* **434,** 898–904
5. Montell, C. (2005) *Sci. STKE* **2005(272),** re3
6. Ramsey, I. S., Delling, M., and Clapham, D. E. (2006) *Annu. Rev. Physiol.* **68,** 619–647
7. Yu, Y., Fantozzi, I., Remillard, C. V., Landsberg, J. W., Kunichika, N., Platoshyn, O., Tigno, D. D., Thistlethwaite, P. A., Rubin, L. J., and Yuan, J. X. (2004) *Proc. Natl. Acad. Sci. U. S. A.* **101,** 13861–13866
8. Maroto, R., Raso, A., Wood, T. G., Kurosky, A., Martinac, B., and Hamill, O. P. (2005) *Nat. Cell Biol.* **7,** 179–185
9. Li, H. S., Xu, X. Z., and Montell, C. (1999) *Neuron* **24,** 261–273
10. Li, Y., Jia, Y. C., Cui, K., Li, N., Zheng, Z. Y., Wang, Y. Z., and Yuan, X. B. (2005) *Nature* **434,** 894–898
11. Richardson, P. M., and Issa, V. M. (1984) *Nature* **309,** 791–793
12. Neumann, S., Skinner, K., and Basbaum, A. I. (2005) *Proc. Natl. Acad. Sci. U. S. A.* **102,** 16848–16852
13. Neumann, S., Bradke, F., Tessier-Lavigne, M., and Basbaum, A. I. (2002) *Neuron* **34,** 885–893
14. Qiu, J., Cai, D., Dai, H., McAtee, M., Hoffman, P. N., Bregman, B. S., and Filbin, M. T. (2002) *Neuron* **34,** 895–903
15. Wu, D., Zhang, Y., Bo, X., Huang, W., Xiao, F., Zhang, X., Miao, T., Magoulas, C., Subang, M. C., and Richardson, P. M. (2007) *Exp. Neurol.* **204,** 66–76
16. Wood, J. N., Bevan, S. J., Coote, P. R., Dunn, P. M., Harmar, A., Hogan, P., Latchman, D. S., Morrison, C., Rougon, G., Theveniau, M., and Wheatley, S. (1990) *Proc. Biol. Sci.* **241,** 187–194
17. Wu, X., Zagranichnaya, T. K., Gurda, G. T., Eves, E. M., and Villereal, M. L. (2004) *J. Biol. Chem.* **279,** 43392–43402
18. Kunert-Keil, C., Bisping, F., Kruger, J., and Brinkmeier, H. (2006) *BMC Genomics* **7,** 159
19. Liu, M., Willmott, N. J., Michael, G. J., and Priestley, J. V. (2004) *Neuroscience* **127,** 659–672
20. Fatherazi, S., Presland, R. B., Belton, C. M., Goodwin, P., Al-Qutub, M., Trbic, Z., Macdonald, G., Schubert, M. M., and Izutsu, K. T. (2007) *Pflugers Arch. Eur. J. Physiol.* **453,** 879–889
21. Leclere, P. G., Norman, E., Groutsi, F., Coffin, R., Mayer, U., Pizzey, J., and Tonge, D. (2007) *J. Neurosci.* **27,** 1190–1199
22. Harper, A. A., and Lawson, S. N. (1985) *J. Physiol.* **359,** 31–46
23. Alvarez, V. A., Ridenour, D. A., and Sabatini, B. L. (2006) *J. Neurosci.* **26,** 7820–7825
24. Costigan, M., Befort, K., Karchewski, L., Griffin, R. S., D'Urso, D., Allchorne, A., Sitarski, J., Mannion, J. W., Pratt, R. E., and Woolf, C. J. (2002) *BMC Neurosci.* **25, 3,** 16
25. Xiao, H. S., Huang, Q. H., Zhang, F. X., Bao, L., Lu, Y. J., Guo, C., Yang, L., Huang, W. J., Fu, G., Xu, S. H., Cheng, X. P., Yan, Q., Zhu, Z. D., Zhang, X., Chen, Z., Han, Z. G., and Zhang, X. (2002) *Proc. Natl. Acad. Sci. U. S. A.* **99,** 8360–8365
26. Tanabe, K., Bonilla, I., Winkles, J. A., and Strittmatter, S. M. (2003) *J. Neurosci.* **23,** 9675–9686
27. Murphy, P. G., Grondin, J., Altares, M., and Richardson, P. M. (1995) *J. Neurosci.* **15,** 5130–5138
28. Murphy, P. G., Borthwick, L. A., Altares, M., Gauldie, J., Kaplan, D., and Richardson, P. M. (2000) *Eur. J. Neurosci.* **12,** 1891–1899
29. Williams, K. L., Rahimtula, M., and Mearow, K. M. (2005) *BMC Neurosci.* **6,** 24
30. Greka, A., Navarro, B., Oancea, E., Duggan, A., and Clapham, D. E. (2003) *Nat. Neurosci.* **6,** 837–845
31. Bezzerides, V. J., Ramsey, I. S., Kotecha, S., Greka, A., and Clapham, D. E. (2004) *Nat. Cell Biol.* **6,** 709–720
32. Tonra, J. R., Curtis, R., Wong, V., Cliffer, K. D., Park, J. S., Timmes, A., Nguyen, T., Lindsay, R. M., Acheson, A., and DiStefano, P. S. (1998) *J. Neurosci.* **18,** 4374–4383
33. Michael, G. J., Averill, S., Shortland, P. J., Yan, Q., and Priestley, J. V. (1999) *Eur. J. Neurosci.* **11,** 3539–3551
34. Agell, N., Bachs, O., Rocamora, N., and Villalonga, P. (2002) *Cell. Signal.* **14,** 649–654
35. Fukuchi, M., Tabuchi, A., and Tsuda, M. (2005) *J. Pharmacol. Sci.* **98,** 212–218
36. Mehta, D., Ahmmed, G. U., Paria, B. C., Holinstat, M., Voyno-Yasenetskaya, T., Tiruppathi, C., Minshall, R. D., and Malik, A. B. (2003) *J. Biol. Chem.* **278,** 33492–33500

37. Haruta, T., Takami, N., Ohmura, M., Misumi, Y., and Ikehara, Y. (1997) *Biochem. J.* **325,** 455–463
38. Lautermilch, N. J., and Spitzer, N. C. (2000) *J. Neurosci.* **20,** 315–325
39. Singh, I., Knezevic, N., Ahmmed, G. U., Kini, V., Malik, A. B., and Mehta, D. (2007) *J. Biol. Chem.* **282,** 7833–7843
40. Laux, T., Fukami, K., Thelen, M., Golub, T., Frey, D., and Caroni, P. (2000) *J. Cell Biol.* **149,** 1455–1472
41. Caroni, P. (2001) *EMBO J.* **20,** 4332–4336
42. Riccio, A., Medhurst, A. D., Mattei, C., Kelsell, R. E., Calver, A. R., Randall, A. D., Benham, C. D., and Pangalos, M. N. (2002) *Brain Res. Mol. Brain Res.* **109,** 95–104
43. Glazebrook, P. A., Schilling, W. P., and Kunze, D. L. (2005) *Pflugers Arch. Eur. J. Physiol.* **451,** 125–130
44. Inada, H., Iida, T., and Tominaga, M. (2006) *Biochem. Biophys. Res. Commun.* **350,** 762–767
45. Huang, W. C., Young, J. S., and Glitsch, M. D. (2007) *Cell Calcium*, **42,** 1–10
46. Strubing, C., Krapivinsky, G., Krapivinsky, L., and Clapham, D. E. (2001) *Neuron* **29,** 645–655
47. Hofmann, T., Schaefer, M., Schultz, G., and Gudermann, T. (2002) *Proc. Natl. Acad. Sci. U. S. A.* **99,** 7461–7466
48. Strubing, C., Krapivinsky, G., Krapivinsky, L., and Clapham, D. E. (2003) *J. Biol. Chem.* **278,** 39014–39019
49. Poteser, M., Graziani, A., Rosker, C., Eder, P., Derler, I., Kahr, H., Zhu, M. X., Romanin, C., and Groschner, K. (2006) *J. Biol. Chem.* **281,** 13588–13595

TRPC4 in Rat Dorsal Root Ganglion Neurons Is Increased after Nerve Injury and Is Necessary for Neurite Outgrowth

Dongsheng Wu, Wenlong Huang, Peter M. Richardson, John V. Priestley and Min Liu

J. Biol. Chem. 2008, 283:416-426.
doi: 10.1074/jbc.M703177200 originally published online October 10, 2007
